SPATIOTEMPORAL STOCHASTIC EFFECTS IN A MODEL OF BISTABLE CHEMICAL SYSTEM

B. NOWAKOWSKI AND A.L. KAWCZYŃSKI

Institute of Physical Chemistry, Polish Academy of Sciences
Kasprzaka 44/52, 01-224 Warsaw, Poland

(Received May 13, 1997)

A simple and realistic model of bistable chemical system in which running fronts can be observed is studied. Mesoscopic characteristics of the model are obtained by numerical simulations of the master equation for spatially distributed system. Velocity of the front and its width obtained in the simulations agree well with the phenonenological description. However, for small diffusion coefficient fluctuations grow locally to a macroscopic size and create pulses. Such effects cannot be described by the phenomenological approach.

PACS numbers: 82.20. Wt, 82.20. Mj, 05.40. +j

Fluctuations can strongly affect dynamics of nonlinear, far-from-equilibrium, chemical systems [1–4]. Such effects can be important if a system is close to a bifurcation. The simplest example is a bistable system close to a saddle-node bifurcation. In this case one of stable stationary states is very close to a saddle point and fluctuations can induce a "jump" of the system from a basin of attraction of this stable stationary state to another one. In the homogenous system only global fluctuations can occur, which change concentrations in the whole volume. The system can be treated as homogeneous either if it is ideally stirred or if its size is so small that diffusion is able to maintain its homogeneity. Analytical solutions for global fluctuations in homogeneous systems are available for the Schlögl model [4].

Different behavior can appear in the unstirred system, in which difusion is unable to disperse small local inhomogeneities. Local fluctuations can form small domains in which concentrations are switched from a basin of attraction of one stationary state to another one. These domains can next grow and cover a macroscopic part of the system. This kind of behavior is studied in the present paper, which extends the previous investigations of

fluctuations in the corresponding homogeneous bistable system [5,6]. We are mainly interested in the influence of diffusion on dynamics of local fluctuations. In particular, we show that sufficiently fast diffusion is able to supress local fluctuations in a system of finite size. On the other hand, if diffusion is decreased local fluctuations can survive and substantially change dynamics of the system. In order to include fluctuations in dynamical description of the system we use the master equation approach which accounts for stochastic character of chemical and transfer processes. A possibility for local fluctuations is included in the master equation for the spatially extended system [1]. Both reaction and diffusion processes are taken into account by this equation.

We consider a chemical scheme the same as in the previous papers [5,6], in which global fluctuations have been studied by various methods. This model is realistic because it consists of elementary reactions only, that is bimolecular reactions excluding autocatalytic steps. These properties of the model allow for its simulations by master equation approach as well as by other techniques, like cellular automata and molecular dynamics methods. Rate constants and diffusion coefficients are chosen in such a way that for apropriate initial conditions the phenomenological description predicts a wave solution in the form of a runnning front. We examine the relation between the stochastic and deterministic descriptions by comparing the results of the master equation approach and the phenomenological solutions for this phenomenon. Stochastic treatment has been already applied to study effect of fluctuations on velocity and width of running chemical front in the simplest model systems [7]. In our paper we focus our attention on spontaneous generation of pulses in regions ahead of the running front or in initially homogeneous systems.

The paper is organized as follows: In Sec. 1 the model is described and its phenomenological dynamics is analyzed. In Sec. 2 the master equation and the algorythm for its simulations are presented. In Sec. 3 the results are presented and discussed.

1. Phenomenological model

The model consists of the following elementary reactions:

$$R + S \underset{k_{-1}}{\overset{k_1}{\rightleftharpoons}} V + S \tag{1}$$

$$V + E \underset{k_{-2}}{\overset{k_2}{\rightleftharpoons}} X + S \tag{2}$$

$$X + S \overset{k_3}{\rightarrow} E + U \tag{3}$$

$$X + V \underset{k_{-4}}{\overset{k_4}{\rightleftharpoons}} Y + S\,. \tag{4}$$

This scheme is a modification of a well known model of an open chemical system with a catalytic (enzymatic) reaction, inhibited by an excess of its reactant V. The reactant V is transformed to the product U with E as the catalyst (steps (2) and (3)). This part of the scheme is the well known Langmuir–Hinshelwood mechanism of catalytic reactions (or the Michaelis–Menten kinetics for enzymatic reactions). Step (4) is the inhibition of the Langmuir–Hinshelwood mechanism (or the Michaelis–Menten scheme) by an excess of the reactant V. It is assumed, that S is a solvent, whose concentration is maintaned constant. The system is open, due to step (1), in which the reactant V is produced from the reagent R, whose concentration is maintained constant. One can arrange such conditions in a continuously fed unstirred reactor (CFUR) or a so called "gel disc reactor". Because we are interested in inhomogenous systems we allow for initial distributions of reagents concentrations which depend on space coordinates. Therefore, local mass balance equations with reaction and diffusion terms for each reagent separately must be used to describe the dynamics of the system. According to the mass action law, the behavior of the system is described by four kinetic equations for V, E, X and Y (because the step (3) is irreversible, the changes of U are determined by concentrations of remaining reactants). For simplicity we restrict our considerations to one dimensional systems.

The kinetic equations have the form:

$$\frac{\partial V}{\partial t} - D_V \frac{\partial^2 V}{\partial x^2} = k_1 RS - k_{-1} VS - k_2 VE + k_{-2} XS - k_4 VX + k_{-4} YS\,, \tag{5}$$

$$\frac{\partial E}{\partial t} - D_E \frac{\partial^2 E}{\partial x^2} = -k_2 VE + (k_{-2} + k_3) XS\,, \tag{6}$$

$$\frac{\partial X}{\partial t} - D_X \frac{\partial^2 X}{\partial x^2} = k_2 VE - (k_{-2} + k_3) XS - k_4 VX + k_{-4} YS\,, \tag{7}$$

$$\frac{\partial Y}{\partial t} - D_Y \frac{\partial^2 Y}{\partial x^2} = k_4 VX - k_{-4} YS\,, \tag{8}$$

where the symbols of the reagents are used to denote their concentrations for convenience, because this notation does not cause any misunderstandings.

In the sequel we will assume that diffusion coefficients of all reagents are identical, and we denote them by D. Moreover, the sum of initial concentration distributions of the catalyst and all its complexes with the reagent

V , that is $E(x,0)+X(x,0)+Y(x,0)$, is constant in space. It is easy to show that in this case the sum: $E(x,t)+X(x,t)+Y(x,t)=E_0$ remains constant for all times $t>0$, and one of the variables (say Y) can be eliminated. Therefore, the dynamics of the system can be described by three reaction-diffusion equations only:

$$\frac{\partial V}{\partial t}-D\frac{\partial^2 V}{\partial x^2} = k_1RS-k_{-1}VS-k_2VE+k_{-2}XS \\ -k_4VX+k_{-4}(E_0-E-X)S, \tag{9}$$

$$\frac{\partial E}{\partial t}-D\frac{\partial^2 E}{\partial x^2} = -k_2VE+(k_{-2}+k_3)XS, \tag{10}$$

$$\frac{\partial X}{\partial t}-D\frac{\partial^2 X}{\partial x^2} = k_2VE-(k_{-2}+k_3)XS \\ -k_4VX+k_{-4}(E_0-E-X)S. \tag{11}$$

Usually, a total concentration of a catalyst (enzyme) E_0 is much smaller than the concentration of the reactant V. In this case one can separate scales of time, in which the concentrations of the reagents change. The variables E and X become then fast variables, whereas V is a slow one. For homogeneous initial distributions of E and X one can assume that their distributions in a slow time scale are equal to their quasistationary values. In this way the fast variables can be eliminated and the dynamics of the system can be described by one kinetic equation for V only:

$$\frac{\partial V}{\partial t}-D\frac{\partial^2 V}{\partial x^2}=k_1RS-k_{-1}VS-\frac{k_3E_0VS}{K_mS+V+V^2/(K_4S)}=f(V), \tag{12}$$

where $K_m=(k_{-2}+k_3)/k_2$ and $K_4=k_{-4}/k_4$.

It is easy to see that for appropriate values of the parameters, there are three values of V for which the right hand side of this equation is equal to zero. These zeros determine the stationary states of the system. It is easy to check that the smallest and the largest ones are stable stationary states whereas the middle one is unstable. Therefore, according to the Kanel's theorem [8] equation (12) with initial condition such that one part of the system is in a basin of attraction of one stable stationary state and the other one is in a basin of attraction of the other stable stationary state, has an asymptotic solution in the form of a running front $V(\xi)$, where $\xi=x\pm\rho t+x_0$.

A velocity of the running front ρ is given by [8–10]:

$$\rho = -\frac{\int_{V_1}^{V_3} f(V)dV}{\int_{-\infty}^{+\infty} \left(\frac{dV}{d\xi}\right)^2 d\xi}. \tag{13}$$

For the particular form of the right hand side of (12) the solution is not known in an explicite form. The sign of ρ is determined by the sign of $\int_{V_1}^{V_3} f(V)dV$. If this integral is positive then the region with V close to V_3 expands and for negative value of the integral the region with V close to V_1 expands.

On the basis of the results for the one variable system we assume that the three variable system (9)–(11) has asymptotic solutions in the form of travelling waves for the three variables provided the right hand sides of (9)–(11) have also three zeros and the variables V, E and X have approprate initial conditions. The validity of this assumption has been confirmed by numerical solutions of (9)–(11).

2. Master equation

The mesoscopic treatment of the spatially distributed (in one dimension) chemical system (1)–(4) is an extension of this approach applied to the corresponding uniform system [5]. The system is divided into (let's say) M cells along the spatial coordinate, the volume Ω and the lenght Δl of each cell are assumed equal. The state of the system is described by probability distribution $P(\{N_{V,i}\}, \{N_{E,i}\}, \{N_{X,i}\}, \{N_{Y,i}\}, t)$ of finding a set of populations $N_{Q,i}$ of species $Q = V, E, X, Y$ in a cell $i = 1, ..., M$. (A number of molecules R, S in each cell is constant, equal to N_R and N_S.) A number of molecules $N_{V,i}, N_{E,i}, N_{X,i}, N_{Y,i}$ in i–th cell can be changed either by a chemical reaction between molecules within a cell or by a transfer of a molecule to/from adjacent cells. Both kind of these processes contribute independently to the time evolution of the distribution function in the spatially distributed system, and the master equation for P can be schematically presented in the form

$$\frac{\partial}{\partial t}P(\{N_{V,i}\}, \{N_{E,i}\}, \{N_{X,i}\}, \{N_{Y,i}\}, t) = \left.\frac{\partial P}{\partial t}\right|_{\text{chem}} + \left.\frac{\partial P}{\partial t}\right|_{\text{diff}}. \tag{14}$$

The contribution due to the chemical processes describes isolated reactions in each single cell provided that populations in other cells remain unchanged; it is a straightforward extension of the corresponding term for the uniform system [5]

$$\begin{aligned}\left.\frac{\partial P}{\partial t}\right|_{\text{chem}} = \sum_{j=1}^{M} \Big(& \kappa_1 N_R N_S P(\ldots, N_{V,j}-1, \ldots, t) \\ & +\kappa_{-1}(N_{V,j}+1) N_S P(\ldots, N_{V,j}+1, \ldots, t) \\ & +\kappa_2 (N_{V,j}+1)(N_{E,j}+1) P(\ldots, N_{V,j}+1, \ldots, N_{E,j}+1, \ldots, t) \\ & +\kappa_{-2}(N_{X,j}+1) N_S P(\ldots, N_{V,j}-1, \ldots, N_{E,j}-1, \ldots, N_{X,j}+1, \ldots, t) \\ & +\kappa_3 (N_{X,j}+1) N_S P(\ldots, N_{E,j}-1, \ldots, N_{X,j}+1, \ldots, t) \\ & +\kappa_4 (N_{V,j}+1)(N_{X,j}+1) P(\ldots, N_{V,j}+1, \ldots, N_{X,j}+1, \ldots, t) \\ & +\kappa_{-4}(N_{Y,j}+1) N_S P(\ldots, N_{Y,j}+1, \ldots, t) \Big) \\ & -\nu_{\text{chem}} P(\{N_{V,i}\}, \{N_{E,i}\}, \{N_{X,i}\}, \{N_{Y,i}\}, t)\,. \end{aligned} \tag{15}$$

On the right hand side, the notation $(\ldots, N_{Q,j}, \ldots)$ means that except $N_{Q,j}$ all populations in the distribution function P remain unchanged. The master equation expresses the rate of change of a probability of a state $(\{N_{V,j}, N_{E,j}, N_{X,j}, N_{Y,j}\})$ as a balance of the 'birth' and 'death' processes. The 'birth' term is formed by the positive components of the right hand side of (14), which describe creation of a given state, resulting from transitions from other states under particular chemical processes (1)–(4). Consequently, the last component of the right hand side of (14) is a 'death' term, describing escape from this state to other points of the configuration space. The coefficient ν_{chem} provides the total rate of escape from the configuration $(\{N_{V,i}\}, \{N_{E,i}\}, \{N_{X,i}\}, \{N_{Y,i}\})$, as a result of chemical reactions

$$\begin{aligned} & \nu_{\text{chem}}(\{N_{V,i}\}, \{N_{E,i}\}, \{N_{X,i}\}, \{N_{Y,i}\}) \\ & = \sum_{j=1}^{M} \Big(\kappa_1 N_R N_S + \kappa_{-1} N_{V,j} N_S + \kappa_2 N_{V,j} N_{E,j} \\ & \quad +(\kappa_{-2}+\kappa_3) N_{X,j} N_S + \kappa_4 N_{X,j} N_{V,j} + \kappa_{-4} N_{Y,j} N_S \Big)\,. \end{aligned} \tag{16}$$

The respective terms of sum (16) represent the rates of reactive collisions, corresponding to reactions (1)–(4). The coefficients κ_i are related to the phenomenological rate constants of bimolecular reactions (1)–(4) by $\kappa_i = k_i/\Omega$. This relation ensures that the chemical terms in the phenomenological equations (5)–(8) can be recovered from the master equation in the limit $\Omega \to \infty$, as the equations for the average number concentrations $\langle N_Q/\Omega \rangle$.

In order to account for the diffusion process it is assumed that every particle can jump with certain probability to a neighbor cell. These hoping rates are related to the diffusion coefficients, and in general can be specific for each species. The term of Eq. (14) describing diffusion has then the following form

$$\begin{aligned}\left.\frac{\partial P}{\partial t}\right|_{\text{diff}} = \sum_{j=1}^{M} \Big(& d_V(N_{V,j-1}+1)P(\ldots,N_{V,j-1}+1,N_{V,j}-1,\ldots,t) \\ & +d_V(N_{V,j+1}+1)P(\ldots,N_{V,j}-1,N_{V,j+1}+1,\ldots,t) \\ & +d_E(N_{E,j-1}+1)P(\ldots,N_{E,j-1}+1,N_{E,j}-1,\ldots,t) \\ & +d_E(N_{E,j+1}+1)P(\ldots,N_{E,j}-1,N_{E,j+1}+1,\ldots,t) \\ & +d_X(N_{X,j-1}+1)P(\ldots,N_{X,j-1}+1,N_{X,j}-1,\ldots,t) \\ & +d_X(N_{X,j+1}+1)P(\ldots,N_{X,j}-1,N_{X,j+1}+1,\ldots,t) \\ & +d_Y(N_{Y,j-1}+1)P(\ldots,N_{Y,j-1}+1,N_{Y,j}-1,\ldots,t) \\ & +d_Y(N_{Y,j+1}+1)P(\ldots,N_{Y,j}-1,N_{Y,j+1}+1,\ldots,t)\Big) \\ & -\nu_{\text{diff}}P(\{N_{V,i}\},\{N_{E,i}\},\{N_{X,i}\},\{N_{Y,i}\},t)\,. \end{aligned} \tag{17}$$

Let us notice, that contrary to the phenomenological description we cannot eliminate the species Y because a number of molecules fluctuates for each component due to diffusion. In the above equation, the terms for boundary cells, $j = 1$ and M, can formally include populations $\{N_{Q,j\pm1}\}$ outside the system, that is for $j = 0$ and $M+1$. The interpretation of these values depends on boundary conditions. If the boundaries of the system are impermeable walls (corresponding to zero-flux boundary conditions in phenomenological description), then transitions of molecules outside the system are forbidden. Consequently, the terms involving $j = 0$ or $M+1$ are disregarded. The coefficient ν_{diff}, describing the total rate of diffusive jumps for all cells, for that system can be written as

$$\begin{aligned}&\nu_{\text{diff}}(\{N_{V,i}\},\{N_{E,i}\},\{N_{X,i}\},\{N_{Y,i}\}) \\ &= d_V N_{V,1} + d_E N_{E,1} + d_X N_{X,1} + d_Y N_{Y,1} \\ &\quad +2\sum_{j=2}^{M-1}\Big(d_V N_{V,j} + d_E N_{E,j} + d_X N_{X,j} + d_Y N_{Y,j}\Big) \\ &\quad +d_V N_{V,M} + d_E N_{E,M} + d_X N_{X,M} + d_Y N_{Y,M}\,. \end{aligned} \tag{18}$$

The relation between the transition rates d_Q and the diffusion coefficients D_Q are obtained from the condition that the usual diffusion terms are recovered from equation (17) in the limit of large volume, $\Omega \to \infty$, and fine division, $\Delta l \to 0$. This yields the equation $d_Q = D_Q/(\Delta l)^2$, which shows that for a

given value of the diffusion coefficient the hoping rates d_Q increase for finer divisions.

The master equation corresponds to the framework of the Fokker–Planck approach, which describes the stochastic system in terms of the probability distribution function. Alternatively, one can use the Langevin approach, in which a stochastic dynamics is considered as a random walk of an individual system. In the case of chemical system considered, it is a random motion in a discrete space, in which coordinates of each point corresponds to a given configuration of populations $\{N_{Q,i}\}$ in cells. We have performed Monte Carlo (MC) simulations of this (continous time) random walk applying the method of Gillespie [11], which generates a stochastic trajectory according to the following algorithm: Let us assume, that the system at an instant t is in a state which is given by the point $(\{N_{V,j}, N_{E,j}, N_{X,j}, N_{Y,j}\})$. The total rate of escape of the system from this point due to any reaction or diffusion process is equal to $\nu = \nu_{\text{chem}} + \nu_{\text{diff}}$. According to this, in the first step of the algorithm, a waiting time τ for the transition is sampled from the exponential distribution

$$\Theta(\tau) = \nu \exp(-\nu\tau)\,. \tag{19}$$

The next step consists in choosing a particular reaction or diffusion process, which causes a transfer of the system to another point. The probability $p(\alpha)$ of selection of process α is proportional to its contribution to the total rate of escape ν. For chemical reaction ρ in a cell j, that means

$$p_{\text{chem}}(\rho, j) = \nu^{-1}\kappa_\rho N_{1\rho,j} N_{2\rho,j}\,, \tag{20}$$

where $N_{1\rho,j}$, $N_{2\rho,j}$ denote populations of molecules of corresponding two species involved in the bimolecular reaction ρ. Similarly, for the probability of a diffusive jump (to the left or right) of a molecule Q in a cell j one obtains

$$p_{\text{diff}}(Q, j) = \nu^{-1} d_Q N_{Q,j}\,. \tag{21}$$

Next, the populations $(\{N_{V,j}, N_{E,j}, N_{X,j}, N_{Y,j}\})$ are updated as they result from the chosen process α; in terms of the random walk the system moves to the new point. Given this new state, generation of the random trajectory proceeds beginning from the first step, and so on.

The coarsed-grained description provided by the master equation, which is based on a division of space in finite size cells, is valid when concentrations in each single cell can be regarded as uniform. This condition can be satisfied if a lenght of a cell is sufficiently small. Using the results of phenomenological approach as a first approximation, this size of a cell can be roughly evaluated from the condition that the relative variation of concentration within a cell is very small. Therefore, the master equation is applicable

if the division is enough fine to describe inhomogenities relevant for a given problem. However, cells resulting from a division must have enough large volume, in order to contain a sufficient number of molecules (at least of the order of ten) to calculate statistics for a single cell, even for reactant of the smallest concentration.

3. Results

In the sequel our main interest is in comparison between the phenomenological description and the master equation approach. While comparing the deterministic and stochastic predictions it is important to realize that simulations of the master equation may be performed for systems with total number of particles of the order of 10^6. Real chemical systems, in which concentrations of reagents are of order of 1 mol/dm^3, cannot have a macroscopic size with such numbers of particles. Consequently, the unit of lenght we use throughtout the paper is 1μm. The unit of time is also rescaled to 10^{-8}s, and then the numerical value of the diffusion coefficient in these units is the same as in cm^2/s. The concentrations are in usual units of mols/dm^3.

Numerical simulations of the master equation can be efficient if concentrations of reagents do not differ by orders of magnitude, because each cell should contain at least a few molecules of a species of the lowest concentration, and at the same time the total number of molecules in a cell should not be too large. Numerical simulations of the master equation introduce also limitations on values of the rate constants. Their ratios should be not too large, because the computer time demanded for simulations is related to the slowest process. The following values of the rate constants are satisfactory from computational point of view: $k_1 = 0.36, k_{-1} = 0.22, k_2 = 2.0$, $k_{-2} = 0.1, k_3 = 3.9, k_4 = 2.0$ and $k_{-4} = 1.0$. The unit of the rate constants is $[(10^{-8}\text{s} \cdot \text{mol/dm}^3)^{-1}]$. Moreover, the following values of the parameters have been selected: $E_0 = 0.2$, $R = 0.5$ and $S = 0.1$. These values of the parameters are the same as in our recent studies of the homogeneous system. For the above values of the rate constants and the parameters the stationary states are determined by:

$$V_1 = 0.113816, \quad E_1 = 0.069820, \quad X_1 = 0.039733 \tag{22}$$

$$V_2 = 0.139666, \quad E_2 = 0.054810, \quad X_2 = 0.038275 \tag{23}$$

$$V_3 = 0.514699, \quad E_3 = 0.006652, \quad X_3 = 0.017120 \tag{24}$$

where (V_1, E_1, X_1), (V_3, E_3, X_3) correspond to the attracting nodes and (V_2, E_2, X_2) corresponds to the saddle point. Let us notice, that the system has a relatively small threshold for an excitation from the first node to the second one. Moreover, the system is close to a bifurcation from the

bistable regime to a monostable one. It is sufficient, for example, to increase the rate constant k_1 by 0.001 to induce a saddle-node bifurcation, in which the first node collapses with the saddle point and both vanish, and the system has one stable stationary state only.

For the above values of the parameters and in a broad range of the diffusion coefficients we verified by numerical solutions of the system (9)–(11) that a region with V_3, E_3 and X_3 expands. In our numerical solutions of (9)–(11) the initial value problem was replaced by the initial-boundary value problem with zero flux boundary conditions at both boundaries of the system. A size of the system was chosen in such a way that the variables at the left end of the system were very close to one stationary state (say V_3, E_3 and X_3) whereas at the right end they are close to V_1, E_1 and X_1. Of course, this procedure is a reasonable approximation of the initial value problem for (9)–(11) if a region in space in which concentrations change from V_1 to V_3 is much smaller than the size of the system and it is far from the each boundary.

The lenght of a cell is uniquely determined by a number of cells used in division of a system of given length. We study the propagation of the chemical trigger wave in the finite system of length $l = 5$ (in μm). The system is initiated in the state (V_3, E_3, X_3) in the interval [0,1] and in the state (V_1, E_1, X_1) in the remaining part. We follow the propagation of the front until it reaches about one half of the system lenght. In MC simulations we tried several division of the system into $M = 200$, 400 and 1000 cells, in order to check if the description by the master equation is correct for the chosen spatial divisions. In order to expect that the master equation approach is valid, it is necesary that the MC results are consistent for all cases, independently of value of M chosen from a given range. In these examinations it was not possible for us to reach finer divisions. The computing time required for simulations increases for larger M, because the rate of diffusive jumps between cells is higher for thiner cells.

In order to study the effect of diffusion on dynamics of the system we used three values of the diffusion coefficient equal to: $5 \cdot 10^{-5}$, $5 \cdot 10^{-4}$ and $5 \cdot 10^{-3}$ (in $\mu m^2/10^{-8}s$). Let us notice that these values correspond to real diffusion coefficients for fluid systems if their units are cm^2s^{-1}. In phenomenological description, faster diffusion leads to increase of both the velocity of the front and its width. Additional effects can be expected in the stochastic description. The faster is diffusion the larger number of cells can be regarded as uniform. Fluctuations which must cover larger domains become less probable. Therefore, diffusion can affect strongly evolution of fluctuations.

Figure 1 shows the snapshots of the moving front, obtained by the numerical solutions of phenomenological equations (9)–(11) with the diffusion coefficient $D = 5 \cdot 10^{-4}$, and by the corresponding MC simulations obtained

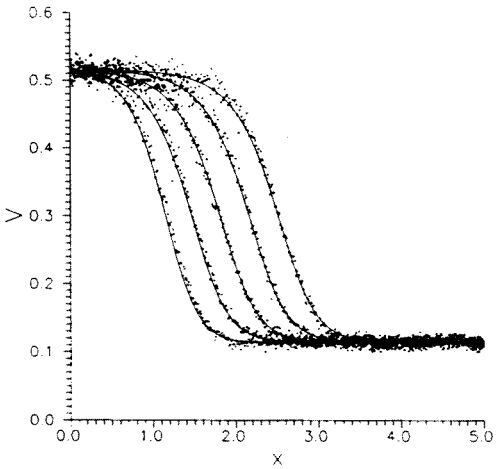

Fig. 1. Spatial distributions of concentration of V for time t = 200, 400, 600, 800, and 1000. The following values of the parameters are used throughout the calculations: $k_1 = 0.36, k_{-1} = 0.22, k_2 = 2.0, k_{-2} = 0.1$, $k_3 = 3.9$, $k_4 = 2.0$, $k_{-4} = 1$, and $E_0 = 0.2, R = 0.5$, $S = 0.1$. The diffusion coefficient $D = 5 \cdot 10^{-4}$. The numerical solutions of the phenomenological equations (9)–(11) are shown in solid line. The simulations of the master equation for $M = 400$, and $\Omega = 8.33 \cdot 10^{-6}$ are shown by dots.

for division into $M = 400$ cells, each of which has volume $\Omega = 8.33 \cdot 10^{-6}$ (all volumes of cells are in μm^3). The results of both methods are quite consistent, indicating that for such volume of cell fluctuations are not very large. The front running from left to right is clearly seen. The similar consistence has been observed also in simulations obtained for the same system partition, except that $\Omega = 2.5 \cdot 10^{-6}$. In the case of this smaller volume of a cell, it has been noticed that patterns obtained in independent simulations are somewhat different due to a stochastic character of the dynamics. In one case a simulated wave front was retarded in comparison to the phenomenological result, whereas in another one it moved somewhat faster. This effect appears because fluctuations increase as volume of a single cell diminishes. Additional simulations performed for $M = 200$ and $\Omega = 5 \cdot 10^{-6}$ exhibited also good agreement with phenomenological results indicating that the master equation with such M and Ω is reasonable.

In a spatially distributed system, fluctuations in individual cells are not independent, because diffusion introduces coupling. The slower is diffusion, this coupling extends over smaller distance. Since relative fluctuations are stronger for smaller volumes, the stochastic effects are more important if

the smoothing effect of diffusion covers smaller domains. This effect can be observed in Figs. 2–5, which show the results for systems with the smaller diffusion coefficient, $D = 5 \cdot 10^{-5}$. The results of the simulations agree well with the deterministic dynamics but fluctuations generate spontaneous pulses in the region ahead of the initial front. This is an essential difference in comparison with the system with the higher diffusion coefficient. After such a pulse is created, it expands according to the wave mechanism and can collapse with the original front. Spontaneous creation of pulses of excitation is a purely stochastic effect which is excluded in the phenomenological description. In Fig. 2 we show the results for $M = 400$ and $\Omega = 8.33 \cdot 10^{-6}$, which correspond to Fig. 1. The front running from

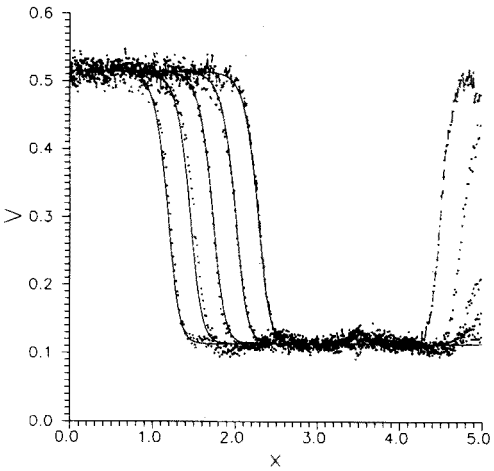

Fig. 2. The same as in Fig. 1, but the diffusion coefficient $D = 5 \cdot 10^{-5}$ and the snapshots are for t=500, 1000, 1500, 2000, and 2500. Phenomenological results are shown in solid line. The MC simulations for $M = 400$ and $\Omega = 8.33 \cdot 10^{-6}$ are shown in dots for the four shorter times, and in dashed line for t=2500.

left to right is more steep as compared with Fig. 1. Beside the front initiated one can observe the spontaneous creation of pulse close to the wall. Figure 3 presents the results for the system with smaller total volume, for the partition $M = 200$, and $\Omega = 5 \cdot 10^{-6}$. In this case fluctuations are more intensive, and the excitations are generated easier than in the previous case. The results shown in Fig. 4 for the same system but with finer division, M=1000 and $\Omega = 10^{-6}$, give the similar evolution of patterns. Figure 5 shows even stronger fluctuations arising in the system with the smaller total volume, that is for M= 200 and $\Omega = 2.5 \cdot 10^{-6}$.

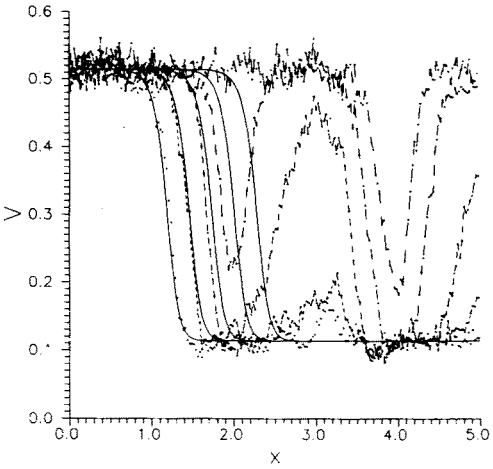

Fig. 3. The same as in Fig. 2 but the MC simulations for $M = 200$ and $\Omega = 5 \cdot 10^{-6}$. The simulations are shown in dots for $t = 500$, in very short dashed line for $t = 1000$, in short dashed line for $t = 1500$, in dashed line for $t = 2000$, and in long dashed line for $t = 2500$.

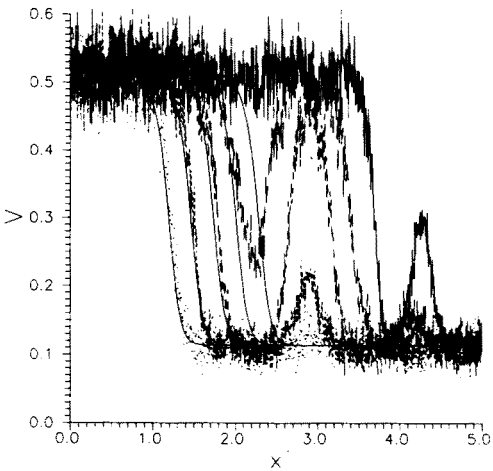

Fig. 4. The same as in Fig. 2 but the MC simulations for $M = 1000$ and $\Omega = 10^{-6}$. The simulations are shown in dots for $t = 500$, in short dashed line for $t = 1000$, in dashed line for $t = 1500$, in long dashed line for $t = 2000$, and in solid line for $t = 2500$.

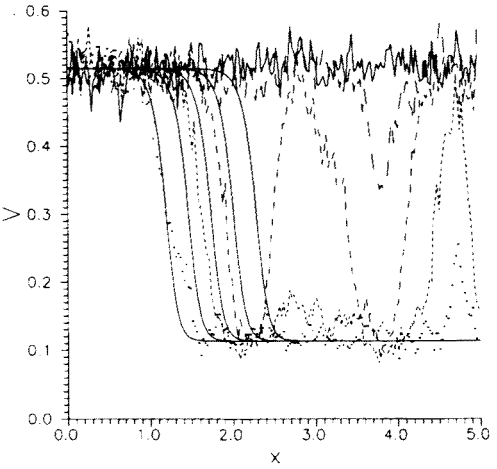

Fig. 5. The same as in Fig. 2 but the MC simulations for $M = 200$ and $\Omega = 2.5 \cdot 10^{-6}$. Phenomenological results are shown in solid line. MC simulations for are shown in dots for $t = 500$, in short dashed line for $t = 1000$, in dashed line for $t = 1500$, in long dashed line for $t = 2000$, and in solid line for $t = 2500$.

According to the deterministic predictions, the front moves faster and becomes wider when the diffusion coefficient is higher. This effect can be observed by comparing Figs. 1, 2 and 6, which depict results for the same system but with different diffusion coefficients $D = 5 \cdot 10^{-5}$, $5 \cdot 10^{-4}$ and $5 \cdot 10^{-3}$, respectively. This trend is also confirmed in stochastic simulations.

Homogeneous system can be excited by local fluctuations, which grow to a macroscopic size by wave expansion mechanism. Figure 7 shows creation of pulse in the initially homogeneous system with diffusion coefficient $D = 5 \cdot 10^{-4}$, for $M = 400$ and $\Omega = 2.5 \cdot 10^{-6}$. The time in which the fluctuation reaches the macroscopic size is much longer than the time in which the front extends over the whole system (compare Fig. 1). For this reason spontaneous generation of pulses have not been observed in systems with the initiated front, for which the longest time of observation is $t = 1000$. For the system with faster diffusion, $D = 5 \cdot 10^{-3}$, the pulses did not appear in homogeneous system for time twice as long as the time of expansion of the wave front (compare Fig. 6). Emergence of spontaneous pulses in the homogeneous system with $D = 5 \cdot 10^{-5}$ is shown in Figs. 8 and 9, for different divisions $M = 400$, $\Omega = 2.5 \cdot 10^{-6}$, and $M = 200$, $\Omega = 5 \cdot 10^{-6}$, respectively. In comparison to the results presented in Fig. 7, the system is excited in a few spots and at much shorter time. It can be noticed in Figs. 8 and 9 that the use of different divisions does not change general features of the results (regardless the stochastic details).

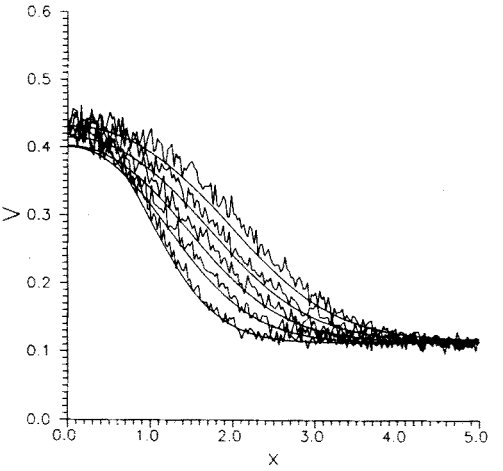

Fig. 6. Spatial distributions of concentration of V for time $t = 60$, 120, 180, 240, and 300. The diffusion coefficient $D = 5 \cdot 10^{-3}$. Both phenomenological results and MC simulations are shown in solid line.

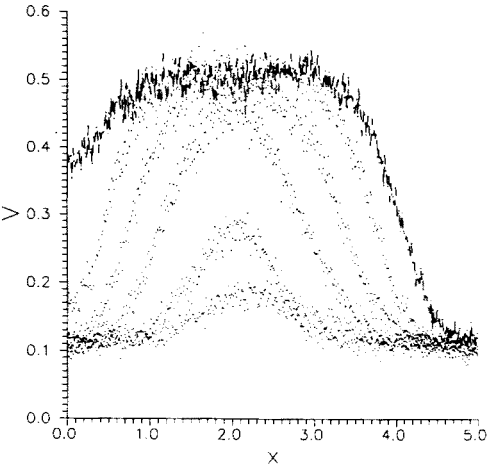

Fig. 7. Spontaneous generation of pulse in the system initially homogeneous at V_1, E_1 and X_1 for $D = 5 \cdot 10^{-4}$. Results of MC simulations for $M = 400$ and $\Omega = 2.5 \cdot 10^{-6}$ are shown for $t = 3700$, 4000, 4300, 4500, 4700, 4900.

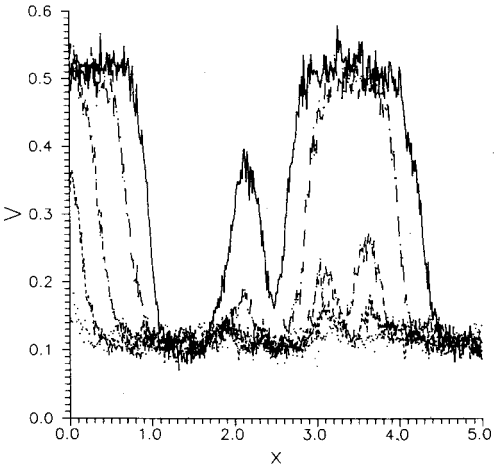

Fig. 8. The same as in Fig. 7 but for $D = 5 \cdot 10^{-5}$. Results of MC simulations for $M = 400$ and $\Omega = 2.5 \cdot 10^{-6}$ are shown as dots for $t = 500$, in short dashed line for $t = 1000$, in dashed line for $t = 1500$, in long dashed line for $t = 2000$, and in solid line for $t = 2500$.

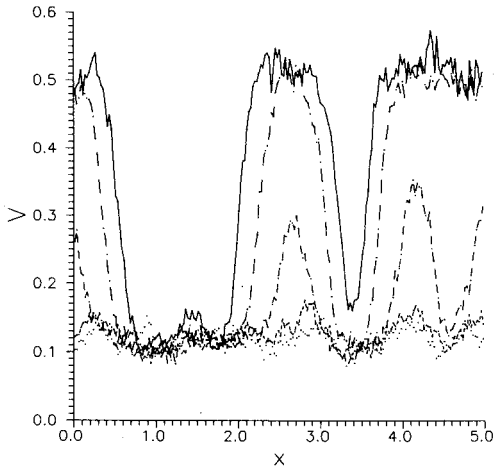

Fig. 9. The same as in Fig. 8 but for $M = 200$ and $\Omega = 5 \cdot 10^{-6}$.

In order to estimate a size of fluctuations which are able to switch the system from the basin of attraction of V_1, E_1 and X_1 to the basin of attraction of V_3, E_3 and X_3 it is useful to consider the reduced system described by (12). Using the linear stability theory one can describe infinitely small

perturbations of the homogeneous stationary states V_1, V_2 and V_3 in the form of normal modes

$$\delta V_i(t,x) = \delta V_{0i} e^{(iqx+\sigma t)}$$

which gives the following relation:

$$\sigma = -Dq^2 + \frac{df(V_i)}{dV}. \tag{25}$$

It is easy to see that if

$$\frac{df(V_i)}{dV} = -k_{-1}S - \frac{k_3 E_0 S[K_m S - V_i^2/(K_4 S)]}{[K_m S + V_i + V_i^2/(K_4 S)]^2} \leq 0$$

then the perturbations with any wave numbers q decay in time. Therefore, the homogeneous stationary states V_1 and V_3 are stable. It is not the case for V_2, for which $df(V_2)/dV \geq 0$ and equals to 0.092958. Thus, for $q \leq q_c = 1/D \cdot df(V_2)/dV$ the value of σ can be positive and the perturbations of the homogeneous state V_2 can grow in time. The critical values of the spatial period $\lambda = 2\pi/q$ for which $\sigma \geq 0$ are equal to 0.145 for $D = 5 \cdot 10^{-5}$ and 0.46 for $D = 5 \cdot 10^{-4}$. These values are rough estimations and they give approximate minimal sizes of fluctuations which can switch the system from the basin of attraction I to III. The results shown in Figs. 7, 8, and 9 confirm

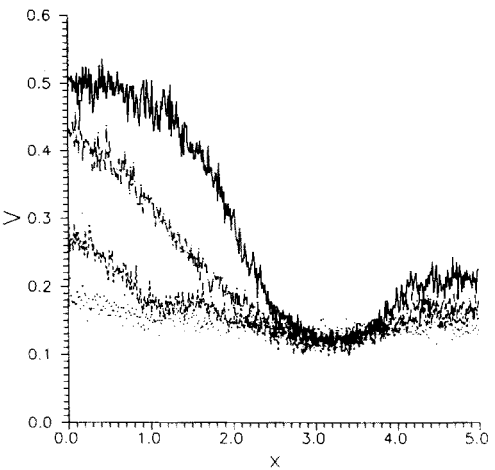

Fig. 10. Spontaneous generation of pulses in the system initially homogeneous at V_2, E_2 and X_2, that is at the saddle point, for $D = 5 \cdot 10^{-4}$. MC simulations for $M = 400$ and $\Omega = 2.5 \cdot 10^{-6}$ are shown for $t = 400$ as dots, for $t = 600$ as the short dashed line, for $t = 800$ as the dashed line, and for $t = 1000$ as the solid line.

these approximate estimations, though in simulations the system is initiated in the stable state I, not in the unstable sadle point II. The evolution of the homogeneous system with $D = 5 \cdot 10^{-4}$ and initiated at the saddle node II is shown in Fig. 10. The size of growing fluctuations is about twice as large as predicted by the above simple estimations.

4. Conclusions

We have demonstrated in the present paper that the master equation can be succesfully applied for description of the spatiotemporal wave phenomena in the multicomponent chemical system. The results of the simulations based on the master equation are consistent with the deterministic dynamics of the system in the case if the stochastic character of the process is not very impotrant. This is the case if diffusion is sufficiently fast to disperse local fluctuations before they reach macroscopic size. However, when fluctuations become comparable with macroscopic quantities, the stochastic effects give rise to the behaviour which cannot be predicted in the framework of the phenomenology. In particular, in the studied bistable system we have observed spontaneous generation of pulses which subsequently expand according to chemical vawe mechanism. The appearance of these pulses substantially

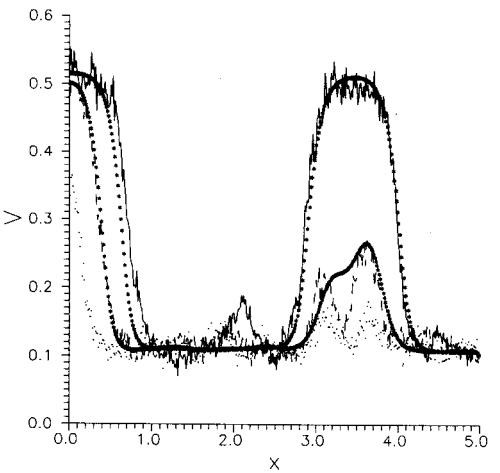

Fig. 11. Spontaneous generation of pulses in the system initially homogeneous at V_1, E_1 and X_1 for $D = 5 \cdot 10^{-5}$. MC simulations for $M = 400$ and $\Omega = 2.5 \cdot 10^{-6}$ are shown at $t = 1000$ (dotted line), 1500 (dashed line), 2000 (solid line). Phenonenological calculations, which used the results of simulations for $t = 1000$ as the initial condition, are plotted as stars.

changes the dynamics of whole system. As can be seen in Fig. 5, the whole system is switched to (V_3, E_3, X_3) in the MC simulations, whereas the running front calculated from the phenomenology covers only about a half of the system. The spontaneous generation of pulses decreases an interval of time necessary to complete the reaction in finite system. It can be noticed that if a pulse reaches sufficiently large magnitude, its subsequent evolution obtained in the MC simulations is quite consistent with dynamics described by the phenomenological approach. An example of such behavior can be seen in Fig. 11, where the distribution obtained in the MC simulation is used as the initial condition for numerical solution of the equations (9)–(11).

This work was financially supported by the grant no. 3 T09A 120 08 provided by the Polish State Committee for Scientific Research.

REFERENCES

[1] G. Nicolis, I. Prigogine, *Self-Organization in Nonequilibrium Systems*, Wiley-Interscience, New York 1977.

[2] C.W. Gardiner, *Handbook of Stochastics Methods for Physics, Chemistry and the Natural Sciences*, Springer, Berlin 1985.

[3] N. van Kampen, *Stochastics Processes in Physics and Chemistry*, North-Holland, Amsterdam 1987.

[4] P.H. Richter, I. Procaccia, J. Ross, *Adv. Chem. Phys.* **43**, 217 (1980).

[5] A.L. Kawczyński, B. Nowakowski, *Pol. J. Chem.* **70**, 1468 (1996).

[6] J. Gorecki, A.L. Kawczyński, B. Nowakowski, *Pol. J. Chem.* **71**, 244 (1997); M. Frankowicz, A.L. Kawczyński, *Pol. J. Chem.* **71**, 467 (1997).

[7] M.A. Karzazi, A. Lemarchand, M. Mareschal, *Phys. Rev.* **E54**, 4888 (1996) and references therein.

[8] Ya.I. Kanel, *Mat. Sbor.* **59**, 243 (1962) (in Russian).

[9] P.C. Fife, *Mathematical Aspects of Reacting and Diffusing Systems*, Springer, Berlin 1979.

[10] A.L. Kawczyński, *Chemical Reactions; from Equilibrium through Dissipative Structures to Chaos*, WN-T, Warsaw 1990 (in Polish).

[11] D.T. Gillespie, *J. Phys. Chem.* **81**, 2340 (1977).